

**AFRL-VA-WP-TP-2006-306**

**OPTIMAL GUIDANCE COMMAND  
GENERATION AND TRACKING  
FOR THE REENTRY OF A  
REUSABLE LAUNCH VEHICLE  
(PREPRINT)**



**Michael W. Oppenheimer  
David D. Doman  
Kevin P. Bollino**

**JANUARY 2006**

**Approved for public release; distribution is unlimited.**

**STINFO FINAL REPORT**

**This work has been submitted to AIAA for publication in the proceedings of the 2006 Guidance, Navigation and Control Conference. If this work is published, this publication is considered a work of the U.S. Government and is not subject to copyright in the United States.**

**AIR VEHICLES DIRECTORATE  
AIR FORCE RESEARCH LABORATORY  
AIR FORCE MATERIEL COMMAND  
WRIGHT-PATTERSON AIR FORCE BASE, OH 45433-7542**

## NOTICE

Using Government drawings, specifications, or other data included in this document for any purpose other than Government procurement does not in any way obligate the U.S. Government. The fact that the Government formulated or supplied the drawings, specifications, or other data does not license the holder or any other person or corporation; or convey any rights or permission to manufacture, use, or sell any patented invention that may relate to them.

This report was cleared for public release by the Air Force Research Laboratory Wright Site (AFRL/WS) Public Affairs Office (PAO) and is releasable to the National Technical Information Service (NTIS). It will be available to the general public, including foreign nationals.

PAO Case Number: AFRL/WS-06-0054, 5 Jan 2006

THIS TECHNICAL REPORT IS APPROVED FOR PUBLICATION.

//ss//

---

Michael W. Oppenheimer  
Electronics Engineer  
Control Design and Analysis Branch  
Air Force Research Laboratory  
Air Vehicles Directorate

//ss//

---

Deborah S. Grismer  
Chief  
Control Design and Analysis Branch  
Air Force Research Laboratory  
Air Vehicles Directorate

//ss//

---

Brian W. Van Vliet  
Chief  
Control Sciences Division  
Air Force Research Laboratory  
Air Vehicles Directorate

This report is published in the interest of scientific and technical information exchange and its publication does not constitute the Government's approval or disapproval of its ideas or findings.

REPORT DOCUMENTATION PAGE				Form Approved OMB No. 0704-0188	
<p>The public reporting burden for this collection of information is estimated to average 1 hour per response, including the time for reviewing instructions, searching existing data sources, gathering and maintaining the data needed, and completing and reviewing the collection of information. Send comments regarding this burden estimate or any other aspect of this collection of information, including suggestions for reducing this burden, to Department of Defense, Washington Headquarters Services, Directorate for Information Operations and Reports (0704-0188), 1215 Jefferson Davis Highway, Suite 1204, Arlington, VA 22202-4302. Respondents should be aware that notwithstanding any other provision of law, no person shall be subject to any penalty for failing to comply with a collection of information if it does not display a currently valid OMB control number. <b>PLEASE DO NOT RETURN YOUR FORM TO THE ABOVE ADDRESS.</b></p>					
1. REPORT DATE (DD-MM-YY) January 2006		2. REPORT TYPE Conference paper preprint		3. DATES COVERED (From - To) 07/20/2005 – 12/21/2005	
4. TITLE AND SUBTITLE OPTIMAL GUIDANCE COMMAND GENERATION AND TRACKING FOR THE REENTRY OF A REUSABLE LAUNCH VEHICLE (PREPRINT)				5a. CONTRACT NUMBER In-House	
				5b. GRANT NUMBER	
				5c. PROGRAM ELEMENT NUMBER N/A	
6. AUTHOR(S) Michael W. Oppenheimer and David D. Doman (AFRL/VACA) Kevin P. Bollino (Naval Postgraduate School)				5d. PROJECT NUMBER N/A	
				5e. TASK NUMBER N/A	
				5f. WORK UNIT NUMBER N/A	
7. PERFORMING ORGANIZATION NAME(S) AND ADDRESS(ES)  Control Design and Analysis Branch (VACA) Control Sciences Division Air Vehicles Directorate Air Force Materiel Command, Air Force Research Laboratory Wright-Patterson AFB, OH 45433-7542				8. PERFORMING ORGANIZATION REPORT NUMBER  AFRL-VA-WP-TP-2006-306	
9. SPONSORING/MONITORING AGENCY NAME(S) AND ADDRESS(ES)  Air Vehicles Directorate Air Force Research Laboratory Air Force Materiel Command Wright-Patterson AFB, OH 45433-7542				10. SPONSORING/MONITORING AGENCY ACRONYM(S) AFRL/VACA	
				11. SPONSORING/MONITORING AGENCY REPORT NUMBER(S) AFRL-VA-WP-TP-2006-306	
12. DISTRIBUTION/AVAILABILITY STATEMENT Approved for public release; distribution is unlimited.					
13. SUPPLEMENTARY NOTES Report contains color. Submitted for publication in the proceedings of the 2006 AIAA Guidance, Navigation and Control Conference. This material is declared a work of the U.S. Government and is not subject to copyright protection in the United States.					
14. ABSTRACT In this work, optimal outer-loop guidance commands are generated from an off-line reference trajectory and then tracked by a reconfigurable inner-loop control law. The primary motivation for this work is a "stepping-stone" towards online, optimal trajectory generation, footprint determination, and retargeting capabilities in the presence of control effector failures or vehicle structural/ aerodynamic degradation, uncertainty, and external disturbances. The presented guidance and control architecture uses a 6-degree-of-freedom simulation and an inner-loop controller to track body-name angular rates (roll, pitch, and yaw), generated from an optimal psuedo-4-degree-of-freedom reference trajectory that is computed using a direct pseudo spectral method. The innerloop control law is capable of reacting and compensating for off-nominal conditions by employing its nonlinear control allocation, dynamic inversion, and model-following/anti-windup prefilters. The results show that the inner-loop control can adequately track the desired optimal guidance commands; thus, confirming the applicability of this control architecture for future development involving on-line, optimal trajectory generation and high-fidelity footprint determination for reentry vehicles.					
15. SUBJECT TERMS Control Theory, Flight Control, Outer-Loop Guidance					
16. SECURITY CLASSIFICATION OF:			17. LIMITATION OF ABSTRACT: SAR	18. NUMBER OF PAGES 34	19a. NAME OF RESPONSIBLE PERSON (Monitor) Michael Oppenheimer 19b. TELEPHONE NUMBER (Include Area Code) (937) 255-8490
a. REPORT Unclassified	b. ABSTRACT Unclassified	c. THIS PAGE Unclassified			

**Optimal Guidance Command Generation and Tracking for the Reentry of a  
Reusable Launch Vehicle \* (PREPRINT)**

Kevin P. Bollino<sup>†</sup>

*Naval Postgraduate School, Monterey, CA 93940*

Michael W. Oppenheimer<sup>‡</sup>

*Air Force Research Laboratory, WPAFB, OH 45433-7531*

David D. Doman<sup>‡‡</sup>

*Air Force Research Laboratory, WPAFB, OH 45433-7531*

**Abstract**

In this work, optimal outer-loop guidance commands are generated from an off-line reference trajectory and then tracked by a reconfigurable inner-loop control law. The primary motivation for this work is a “stepping-stone” towards online, optimal trajectory generation, footprint determination, and retargeting capabilities in the presence of control effector failures or vehicle structural/aerodynamic degradation, uncertainty, and external disturbances. The presented guidance and control architecture uses a 6-degree-of-freedom simulation and an inner-loop controller to track body-frame angular rates (roll, pitch, and yaw), generated from an optimal pseudo-4-degree-of-freedom reference trajectory that is computed using a direct pseudospectral method. The inner-loop control law is capable of reacting and compensating for off-nominal conditions by employing its nonlinear control allocation, dynamic inversion, and model-following/anti-windup prefilters. The results show that the inner-loop control can adequately track the desired optimal guidance commands; thus, confirming the applicability of this control architecture for future development involving on-line, optimal trajectory generation and high-fidelity footprint determination for reentry vehicles.

---

\*This material is declared a work of the U.S. Government and is not subject to copyright protection in the United States.

<sup>†</sup>Ph.D. Candidate, Department of Mechanical and Astronautical Engineering, Guidance, Navigation, and Control Lab, Ph. 831-656-3183, Email: [kpbollin@nps.edu](mailto:kpbollin@nps.edu), AIAA Member.

<sup>‡</sup>Electronics Engineer, 2210 Eighth Street, Bldg. 146, Rm. 305, Ph. 937-255-8490, Email: Michael.[Oppenheimer@wpafb.af.mil](mailto:Oppenheimer@wpafb.af.mil), AIAA Member.

<sup>‡‡</sup>Senior Aerospace Engineer, 2210 Eighth Street, Bldg. 146, Rm. 305, Ph. 937-255-8451, Email: [David.Doman@wpafb.af.mil](mailto:David.Doman@wpafb.af.mil), Senior AIAA Member

## 1. Introduction

The safety of manned or unmanned space vehicles returning to earth is of paramount importance. One way to improve their safety is by creating more capable, reliable and efficient guidance, navigation, and control methods. Onboard, real-time optimal trajectory generation, planning, adaptation, reconfiguration, and retargeting are the methods currently being pursued to achieve the autonomous operations needed to facilitate the accomplishment of these objectives.

Previous work by Shaffer [1]-[2] has integrated trajectory reshaping and retargeting with the reconfigurable control work of Oppenheimer et al. [3]-[5], to demonstrate relatively fast computations of optimal trajectories under trim deficient path-constraints. This work used interpolated aerodynamic data that incorporated wing, body and trim effects from a given vehicle flight condition and an optimized effector displacement vector [2]. This essentially decoupled the outer loop from the inner loop. Despite efforts involving on-line approaches [6]-[11], off-line reference trajectories are still used for tracking applications. Since the early days of space shuttle entry guidance, designers have been employing various reference trajectory tracking schemes [12]. Various research has addressed the reentry problem by using an optimal trajectory generator to solve for a reference input trajectory off-line, then use other inner-loop control means to track the desired trajectory [13]-[15]. In some cases, off-line reference trajectories are combined with on-line trajectory generators such as the “Optimum-Path-To-Go” methodology developed by Schierman et al., as previously cited.

In a similar fashion, this paper combines some of the approaches mentioned to demonstrate that a previously developed inner-loop control design based on dynamic inversion can successfully track variable body-axis roll, pitch, and yaw commands generated from an off-line, optimal reference trajectory. For this work, a full, 6-degree-of-freedom (DOF) model of a reusable launch vehicle (RLV) was employed for the inner-loop tracking simulation whereas the reference trajectory was generated using a psuedo-4-DOF model. The reference trajectory uses a rapid, direct method that has the potential for on-line applications such as the optimal nonlinear feedback approach demonstrated in [16].

To solve the optimal control problem, a spectral algorithm [17]-[19] known as the Legendre Pseudospectral Method is employed by use of a MATLAB-based software package called DIDO [20]. This direct method discretizes the problem and approximates the states, co-states and control variables by use of Lagrange interpolating polynomials where the unknown coefficient values coincide with the Legendre-Gauss-Lobatto (LGL) node points. After this approximation step, a nonlinear programming program (NLP) solver (SNOPT) solves a sequence of finite-dimensional optimization problems that capture the nonlinearities of the system in the form of an optimal control problem. For an extensive description of this method and its use for reentry applications, see references [1]-[2], [16], and [17]-[22].

The purpose of this work is based on various components leading to the development of high-fidelity footprint generation. The following list identifies the specific objectives for this study.

1. To see how well the inner-loop controller tracks the DIDO (optimal) command histories and identify any problems

2. To verify what the body-frame angular rates (P,Q,R) should be (steady-state trim values?) since previously assumed constant in other studies
3. To generate initial guesses for 6-DOF DIDO model (Note: Not required unless real-time implementation is desired)
4. To eventually compare 6-DOF simulation control deflection histories to optimal deflections computed by a 6-DOF DIDO model in order to make generalizations about inner/outer loop interactions/conflicts and determine better cost functions for the control allocator
5. To eventually compare DIDO's 6-DOF "integrated" G&C states to PQR-Tracking "separated" G&C states to confirm conjecture regarding "integrated" G&C feasibility

### 3. Guidance and Control Design Architecture

The overall guidance and control design architecture for this work is presented in Fig. 1 below. As seen, the architecture consists of a two-loop structure: (1) an outer loop that compares the actual angle-of-attack and the bank angle measurements with those provided from the optimal reference trajectory outputs and (2) an inner-loop that is designed to track the optimal body-rates (p,q,r) generated from the guidance command generator.

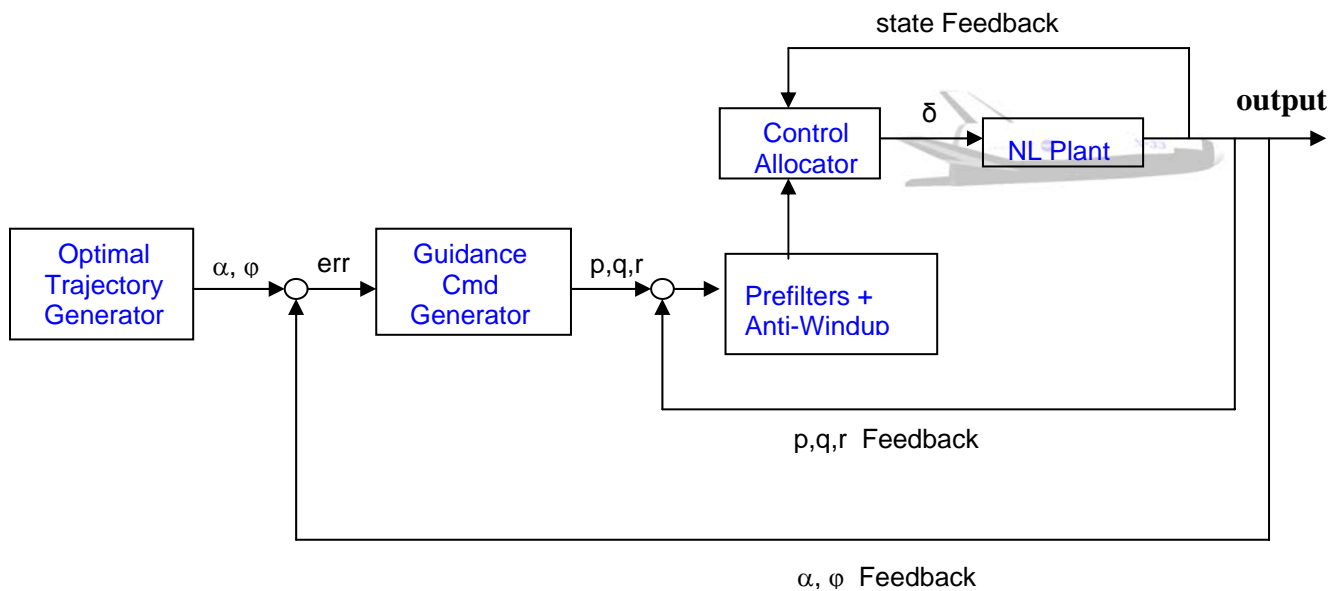


**Fig. 1: Overview of G&C Design Architecture**

## 4. Outer-Loop Guidance Command Generation

### 4.1. Off-Line, Optimal Trajectory Generation

First, an off-line reference trajectory is generated by posing the reentry problem into a standard nonlinear programming fashion and solving for the optimal controls using a direct Legendre pseudospectral method. For this paper, a reduced-order model is adequate to demonstrate the feasibility of the approach. Thus, the full 6-DOF equations of motion are simplified and

decoupled. The model used here assumes a point-mass-model over a flat, non-rotating earth such that the positional and translational equations of motion in a Cartesian “local horizontal” coordinate system become

$$\begin{aligned}
\dot{x} &= V \cos \beta \cos \gamma \\
\dot{y} &= V \sin \beta \cos \gamma \\
\dot{z} &= V \sin \gamma \\
\dot{V} &= -\frac{D}{m} - g \sin \gamma \\
\dot{\gamma} &= \frac{L}{mV} - \frac{g \cos \gamma}{V} \\
\dot{\psi} &= \frac{L \sin \phi}{mV \cos \gamma}
\end{aligned} \tag{1}$$

where  $x$  (down-range),  $y$  (cross-range), and  $z$  (altitude) are the vehicle’s position with respect to the fixed-earth reference frame,  $V$  is the velocity magnitude (i.e. total equivalent airspeed),  $\gamma$  is the flight-path-angle (FPA),  $\psi$  is the azimuth angle,  $\alpha$  is the angle-of-attack (AoA),  $\phi$  is the angle-of-bank (AoB),  $\beta$  is the sideslip angle, and  $m$  is the vehicle’s approximate mass during reentry modeled as 2455 slug ( $\sim 79,000$  lbs).

The lift and drag forces are represented as  $L$  and  $D$ , respectively, and are given by

$$L = \frac{1}{2} \rho V^2 C_L S_{ref} \tag{2}$$

$$D = \frac{1}{2} \rho V^2 C_D S_{ref} \tag{3}$$

where  $S_{ref} = 1600 \text{ ft}^2$  is the aerodynamic reference area. The aerodynamic coefficients are assumed to be functions of state variables only:

$$C_L, C_D = f(\alpha, M) \tag{4}$$

and the Mach number and atmospheric density are functions of altitude:

$$M = M(z) \tag{5}$$

$$\rho = \rho(z) \tag{6}$$

The lift and drag coefficients are computed using table lookup data that incorporates wing, body, and trim effects. Likewise, the Mach and density are computed using table lookup data based on a standard 1976 atmospheric model. See Ref. [2] for more details on the use of table lookup data for a similar model.

The controls to be optimized for this problem are essentially the standard AoA and AoB modulation, but to help compensate for command delays (i.e. lags) and to add more realism/fidelity to the problem, as explained in Ref. [1] and [2], the rates of these angles are used

as “virtual” controls. This has the benefit of allowing rate limits on AoA and AoB which prevents unrealistic responses. Therefore, the control vector is defined as

$$\underline{u} = [\dot{\alpha} \quad \dot{\phi}]^T \in \Re^2 \quad (7)$$

and the state vector is

$$\underline{x} = [x \quad y \quad z \quad V \quad \gamma \quad \psi \quad \alpha \quad \theta]^T \in \Re^8 \quad (8)$$

As with any dynamical optimization problem, the cost function (objective function), governing equations of motions, path constraints, boundary limits on initial/final conditions, and any constraints (on states and/or controls) must be defined. As such, the general optimal control problem for trajectory generation is fully posed in the following manner:

$$\begin{aligned} \min_u J(\underline{x}(\tau), \underline{u}(\tau), \tau_0, \tau_f) &= E(\underline{x}(\tau_0), \underline{x}(\tau_f), \tau_0, \tau_f) + \int_{\tau_0}^{\tau_f} F(\underline{x}(\tau), \underline{u}(\tau), \tau) d\tau \\ \text{subject to} \quad \dot{\underline{x}} &= \underline{f}(\underline{x}, \underline{u}, \tau) \\ \underline{h}_l &\leq \underline{h}(\underline{x}, \underline{u}, \tau) \leq \underline{h}_u \\ \underline{e}_l &\leq \underline{e}(\underline{x}(\tau_0), \underline{x}(\tau_f), \tau_0, \tau_f) \leq \underline{e}_u \\ \underline{x}_l &\leq \underline{x}(\tau) \leq \underline{x}_u \\ \underline{u}_l &\leq \underline{u}(\tau) \leq \underline{u}_u \end{aligned} \quad (9)$$

The goal is to find a state-control function pair,  $\{x(\cdot), u(\cdot)\}$ , or sometimes time,  $\tau$ , that minimizes the performance index represented by the Bolza form,  $J(\cdot)$ , consisting of either a Mayer term,  $E(\cdot)$ , a Lagrange term,  $F(\cdot)$ , or both as stated above.

Summarizing the previous reentry equations, the specific optimal control formulation for this RLV problem is stated as follows: Given an initial position vector  $([x_0, y_0, z_0])$ , velocity magnitude  $(V_0)$ , FPA  $(\gamma_0)$ , heading angle  $(\psi_0)$ , AoA  $(\alpha_0)$ , and AoB  $(\phi_0)$ , find the control history  $(\dot{\alpha}, \dot{\phi})$  that maximizes the horizontal downrange  $(x_f)$  or cross-range  $(y_f)$  under various constraints.

In the context of equation of (9) above and for the analysis presented in this work, the cost functions are simply:

$$\text{Min} \{ J[\cdot] = -x_f \} \quad - \text{ or } - \quad \text{Min} \{ J[\cdot] = -y_f \} \quad (10)$$

subject to the dynamic constraints given by those equations in (1), the initial and final event conditions specified as:

$$(t_0, x_0, y_0, z_0, V_0, \gamma_0, \psi_0, \alpha_0, \phi_0) = (0, 0, 0, 125000 \text{ ft}, 5714 \frac{\text{ft}}{\text{s}}, -1.3 \text{ deg}, 0, 0 \text{ deg}, 0) \quad (11)$$

$$(h_f, V_f) = (500 \text{ ft}, 335 \frac{\text{ft}}{\text{s}}) \quad (12)$$

$$-25 \frac{\text{ft}}{\text{s}} \leq \dot{z}_f \leq 8.33 \frac{\text{ft}}{\text{s}} \quad (13)$$

and the state (14), path (15), and control (16) inequality constraints, respectively, specified as

$$\begin{bmatrix} 0 \\ -\infty \\ 0 \\ 0 \\ -90 \text{ deg} \\ -90 \text{ deg} \\ -10 \text{ deg} \\ -90 \text{ deg} \end{bmatrix} \leq \begin{bmatrix} x \\ y \\ z \\ V \\ \gamma \\ \psi \\ \alpha \\ \phi \end{bmatrix} \leq \begin{bmatrix} \infty \\ \infty \\ \infty \\ \infty \\ 90 \text{ deg} \\ 90 \text{ deg} \\ 50 \text{ deg} \\ 90 \text{ deg} \end{bmatrix} \quad (14)$$

$$\begin{bmatrix} -2.5 \text{ g's} \\ 0 \\ 0 \end{bmatrix} \leq \begin{bmatrix} n_z \\ \bar{q} \\ Q \end{bmatrix} \leq \begin{bmatrix} 2.5 \text{ g's} \\ 600 \frac{\text{lb}}{\text{ft}^2} \\ 60 \frac{\text{BTU}}{\text{ft-s}} \end{bmatrix} \quad (15)$$

$$-40 \frac{\text{deg}}{\text{s}} \leq u_\alpha, u_\phi \leq 40 \frac{\text{deg}}{\text{s}} \quad (16)$$

## 4.2. On-Line Optimal Trajectory Generation

Although this work computes the optimal reference trajectory off-line and then extracts the appropriate signals to use in the guidance command generation algorithm, preliminary studies conducted concurrently with this work have indicated that the same model using approximated

aerodynamic data can solve the problem approximately 85 % faster than using the table look-up data. For example, recent work used a second-order polynomial approximation for lift and drag coefficients and a standard two-parameter exponential atmospheric model that resulted in the successful implementation of a nonlinear sampled-data feedback method with an on-line, trajectory re-optimization scheme that could generate optimal trajectories 99.75 % faster than the same model using the table look-up data [16]. Further work is required to improve the accuracy of the approximations, but initial results look promising for on-line reentry applications.

#### 4.3. P,Q,R Command Generation via “Backstepping Architecture” (PI & DI)

From the optimal trajectory, the  $\alpha$  and  $\phi$  commands are converted into the body-axis angular velocities (P, Q, R) to provide the desired inner-loop commands. The generation of these commands is based on what Schierman defines as a “backstepping” approach whereby the “pseudo-commands” at each loop-closure using proportional-integral (PI) control and dynamic inversion (DI) drives the next inner-most loop [23]. Common loop closures may consist of an outer-most altitude loop, a FPA loop, and an enclosed inner-most AoA loop. For this experiment, the 3-DoF DIDO trajectory provides the  $\alpha$  and  $\phi$  commands that are then used to generate the body-rate commands (P, Q, R). For example, assuming only longitudinal guidance, the appropriate pitch rate command is generated based on the following calculations.

Assuming only longitudinal motion and ignoring later-directional influences (for now), the wind-axis relation  $\alpha = \theta - \gamma$  and the simplified pitch rate  $Q = \dot{\theta}$  provide the governing equation of motion such that

$$\dot{\alpha} = -\dot{\gamma} + Q \quad (17)$$

Also, the governing equation of motion for the FPA is

$$\dot{\gamma} = \frac{L}{mV} - \frac{g \cos(\theta)}{V} \quad (18)$$

Substituting eqn. (17) into eqn. (18), the resulting Q-command is derived as

$$Q_{cmd} = \dot{\alpha}_{des} + \frac{L}{mV} - \frac{g \cos(\gamma)}{V} \quad (19)$$

To improve  $\alpha$  tracking, the desired  $\alpha$  dynamics are generated using a proportional feedback controller

$$\dot{\alpha}_{des} = K_{\alpha}(\alpha_{cmd} - \alpha) \quad (20)$$

where  $\alpha_{cmd}$  is the optimal  $\alpha$  command from the 3-DoF DIDO trajectory.

Figure 2 shows a block diagram that represents the computation of the optimal guidance commands.

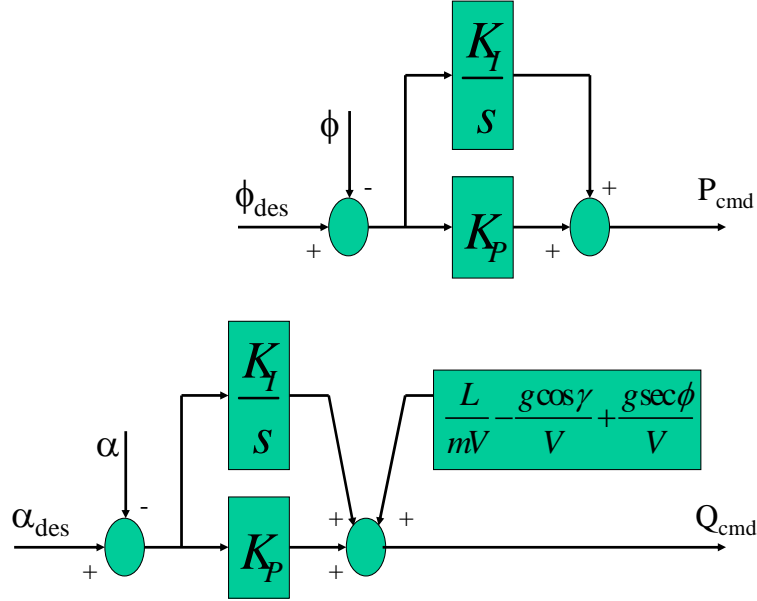


**Fig. 2: P and Q Command Generation**

Note that for the pitch command generation ( $Q_{cmd}$ ) in Fig. 2, an extra lateral term is added to account for lateral effects as explained in the results section. Also, not shown in Fig. 2, is the generation of the yaw command ( $R_{cmd}$ ) that is computed according to Ref. [27] assuming coordinated turns and is given by

$$R_{cmd} = P_{cmd} \tan \alpha + \frac{g \sin \phi}{u} \quad (21)$$

## 5. Reconfigurable Inner-Loop Control

This work implemented a 6-DOF simulation containing a reconfigurable inner-loop control algorithm that consists of dynamic inversion, control allocation, and model following prefilters with integrator anti-windup and reference model bandwidth attenuation

### 5.1. Dynamic Inversion and Control Allocation

The inner-loop control system uses dynamic inversion in order to track the desired body-frame angular velocities  $(p_{des}, q_{des}, r_{des})$ . The rotational dynamics for this type of vehicle can be written as:

$$(22)$$

$$I\dot{\omega} = G_B - \omega \times I\omega$$

where  $I$  is the moment-of-inertia tensor,  $\omega = [p, q, r]^T$ , and  $G_B$  is a vector consisting of the total moments acting on the vehicle with contributions from the wing-body-propulsion system (BAE) and the control effectors ( $\delta$ ) such that

$$G_B = G_{BAE}(\omega, P) + G_\delta(P, \delta) = \begin{bmatrix} L \\ M \\ N \end{bmatrix}_{BAE} + \begin{bmatrix} L \\ M \\ N \end{bmatrix}_\delta \quad (23)$$

where L,M,N are the rolling, pitching, and yawing moments, respectively, the vector  $P$  denotes a measurable or estimable quantity that can influence body rates and can contain variables such as AoA, sideslip, Mach number, and mass properties, and  $\delta$  is a vector of control surface deflections given by  $\delta = [\delta_1, \delta_2, \dots, \delta_n]^T$ . To design the dynamic inversion control law, the equations above are put into a more standard form by defining  $f(\omega, P) \triangleq G_{BAE}(\omega, P) - \omega \times I\omega$  such that

$$I\dot{\omega} = f(\omega, P) + G(P, \delta) \quad (24)$$

The objective is to find a control law that provides direct control over  $\dot{\omega}$  such that  $\dot{\omega} = \dot{\omega}_{des}$ ; therefore, the dynamic inversion control law must satisfy

$$I\dot{\omega}_{des} - f(\omega, P) = G(P, \delta) \quad (25)$$

But, since this problem has more control effectors than control variables, a control allocation algorithm is required for a unique solution. A linear programming based control allocator, which obeys rate and position limits, will be used in this work. In order to implement this type of allocator, the control dependent portion of Eq. (25) must be linear in the controls. Hence, Eq. (25) is rewritten as

$$\dot{\mathbf{I}}\omega_{des} - \mathbf{f}(\omega, \mathbf{P}) = \mathbf{G}(\mathbf{P}, \delta) = \tilde{\mathbf{G}}(\mathbf{P})\delta \quad (26)$$

In order to account for nonlinearities in the moment-deflection relationship, a slope-intercept term is added to Eq. (26) such that

$$\dot{\mathbf{I}}\omega_{des} - \mathbf{f}(\omega, \mathbf{P}) = \tilde{\mathbf{G}}(\mathbf{P})\delta + \epsilon(\mathbf{P}, \delta) \quad (27)$$

Then, the final inverse control law becomes

$$\dot{\omega}_{des} - f(\omega, P) - I^{-1}\epsilon(P, \delta) = I^{-1}\tilde{G}_\delta(P)\delta \quad (28)$$

For more details on this dynamic inversion method and the control allocation algorithm see references [3]-[5] and [23]-[25]. A block diagram representation of the dynamic inversion control law is shown in Fig. 3.

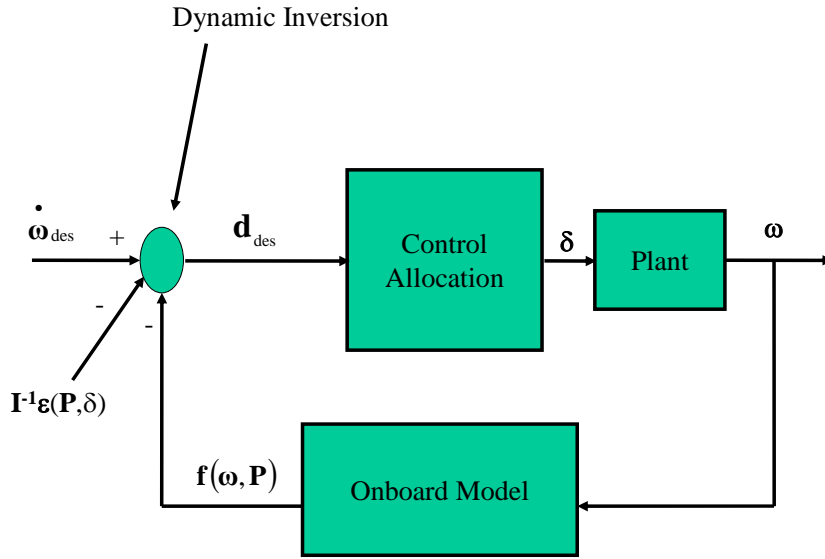


**Fig. 3: Dynamic Inversion with Control Allocation**

### 5.3. Model Following Prefilters

To provide robustness to modeling errors, inversion errors, and to help shape the closed-loop response, prefilters were added to the dynamic inversion control system previously described. Previous work involving the inner-loop control designs for the X-40A tested two different prefilter structures: implicit [4] and explicit [23]. For this work, an implicit model-following scheme was selected based on its simplicity in regards to having fewer gains that would ultimately need tuning. Also, it was desired that the closed-inner-loop control system from  $\omega_{des}$  to  $\omega$  has the characteristics of a first-order response. The implicit structure presented in Fig. 5 provides this behavior and helps compensate for imperfections in the dynamic inversion control law. A closer look at this structure with some straight-forward block diagram algebra reveals that a stable pole/zero cancellation occurs. The resulting transfer function displays the desired closed-inner-loop response:

$$\frac{\omega}{\omega_{des}} = \frac{\frac{K_b}{2}}{s + \frac{K_b}{2}} \quad (29)$$

Note that Fig. 5 only displays a single loop; however, the actual model implemented contained a loop for each of the body-axis angular rates.

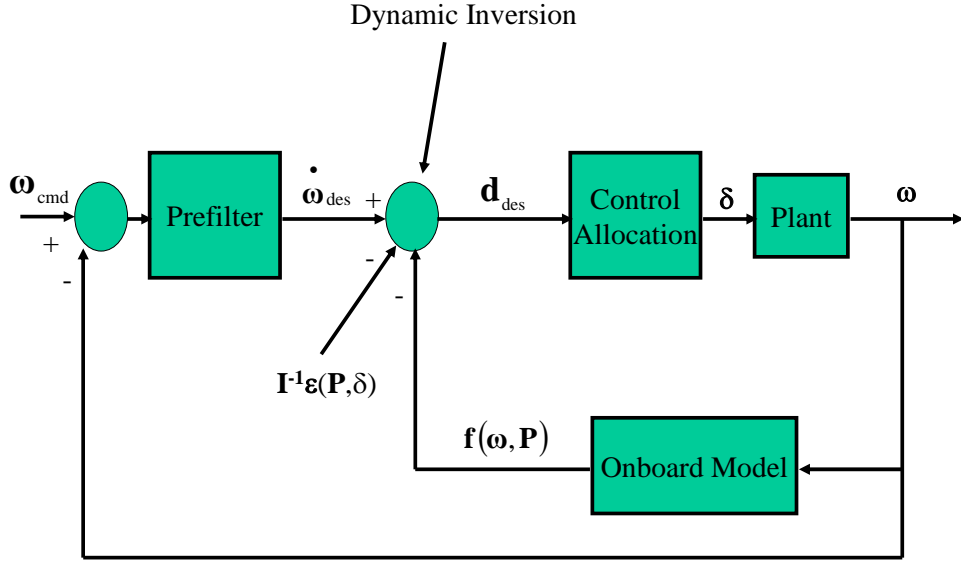


**Fig. 4: Dynamic Inversion with Control Allocation and Prefilters**

#### 5.4. Integrator Anti-Windup and Reference Model Bandwidth Attenuation

Axis saturation occurs when all control power is used on one or more axes. For flight control applications, when a control surface moves at its rate limit or resides on a position limit, then control effector saturation occurs. This is a necessary, but not sufficient, situation for axis saturation. With axis saturation, no additional control power is available when requested by the control system and this should be taken into account by the control law. Analysis of the control allocation inputs ( $\mathbf{d}_{des}$ ) and outputs ( $\mathbf{B}\delta$ ) can indicate axis saturation. To prevent canceling tracking errors caused by the axis saturation, the following integrator anti-windup law is added to reduce the magnitude of input signal to the integrator.

$$I_{AW} = K_{AW} (B\delta_{cmd} - d_{des}) \quad (30)$$

where  $K_{AW}$  is the anti-windup gain,  $d_{des}$  is the desired accelerations from the control effectors, and  $B\delta_{cmd}$  is what the control allocator thinks is being produced by the effectors. If no saturation

occurs, then  $B\delta_{cmd} - d_{des} = 0$  and the control law operates normally; otherwise, at least one axis is saturated and the state of the prefilter integrator is reduced by the anti-windup signal. The anti-windup scheme is implemented as depicted in Fig. 5. For more details on the anti-windup integrator and its use see Ref. [26] and [23].

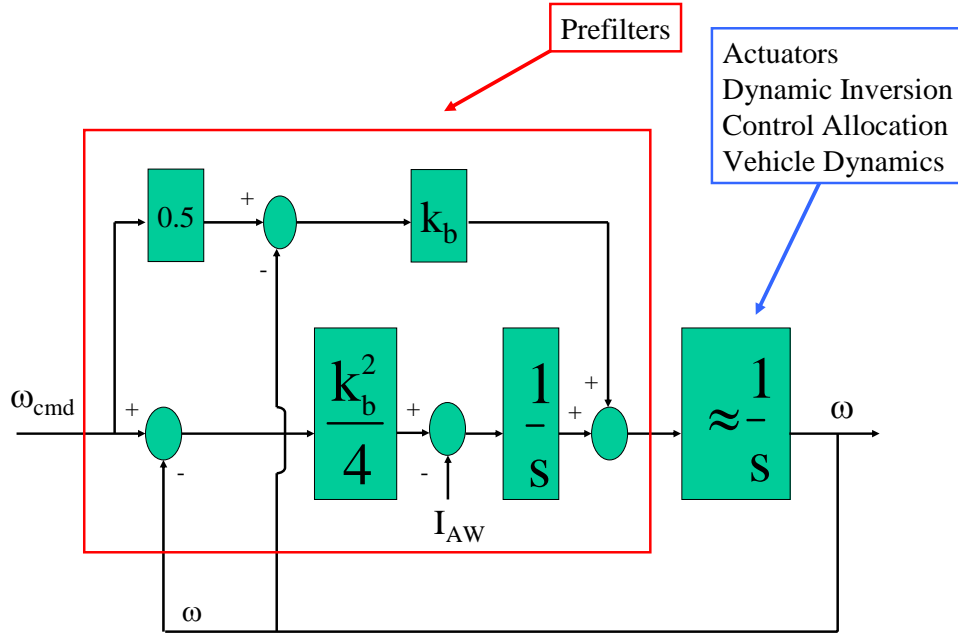


**Fig. 5: Implicit Model Following Prefilter Integrator Anti-Windup Compensation**

## 6. Results and Discussions

The primary performance concerns for this work were tracking error and control saturation. Of course the overall index of performance is that the cost functions for both the outer-loop guidance and inner-loop control agree to within an acceptable tolerance. As long as the desired trajectory and cost were accomplished, the tracking performance was only graphically confirmed.

For this paper, only the max downrange and max cross-range results are presented.

### 6.1. Max Downrange (DR) Case

For the case of maximizing the vehicle's downrange distance, the 3-DOF optimal trajectory is generated off-line and  $\alpha$  and  $\phi$  histories are extracted for use as the desired guidance commands. These commands are shown in Fig. 6.

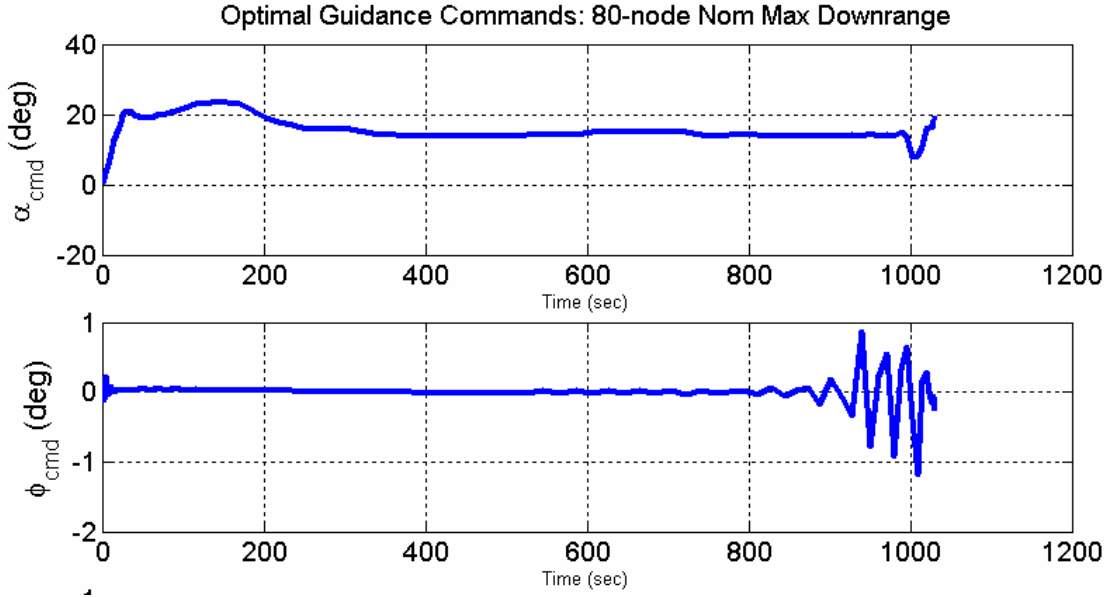


**Fig. 6: Max DR Commands from 3-DOF Optimal Reference Trajectory**

Initial comparison of the PQR-guidance commands with the actual PQR-states revealed that the inner-loop controller was successfully tracking the desired values; however, when comparing the actual states to those of the reference trajectory, there were some unacceptable errors, especially for  $\alpha$ . After carefully reviewing the data, trial-and-error gain tuning on the prefilter and anti-windup gains, it was determined that adding an integrator in the command generation block improves the reference trajectory tracking as seen from comparing Fig. 7 with Fig. 8.

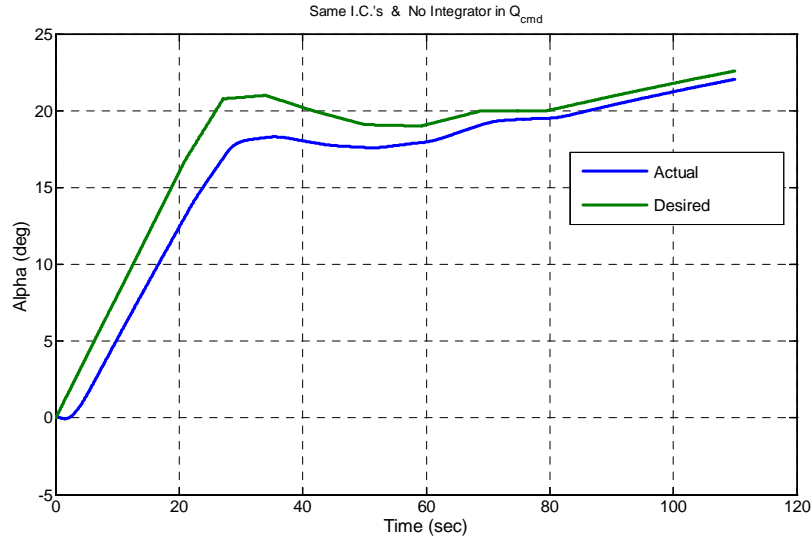


**Fig. 7: AoA WITHOUT Integrator in Command Generation Logic**

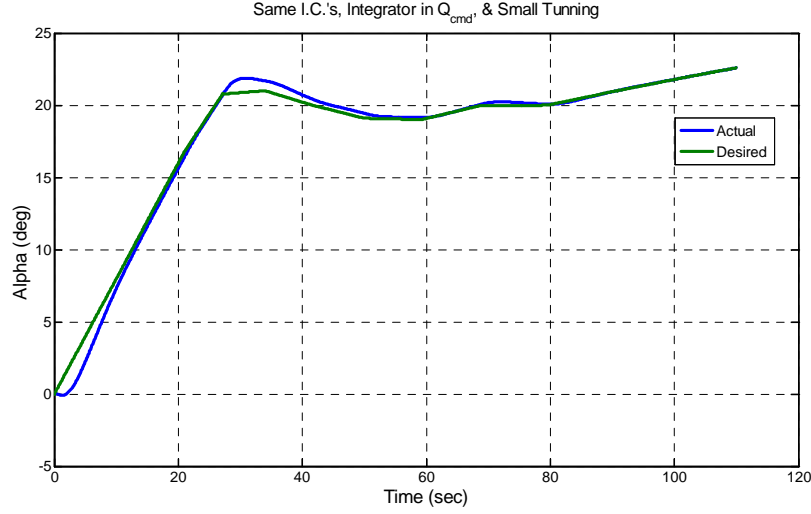


**Fig. 8: AoA WITH Integrator in Command Generation Logic**

With this addition and use of the gains in Table 1, the max DR results presented in Fig. 9 through Fig. 17 were acceptable with an average difference of only 2 %. The cost for the optimal reference trajectory and the simulation were 1,515,588 ft and 1,515,852 ft, respectively, which results in only a 0.017 % error.

	Max DR	Max CR
<b>Prefilter BW, P (<math>K_{bP}</math>)</b>	5.0	4.0
<b>Prefilter BW, Q (<math>K_{bQ}</math>)</b>	5.0	4.0
<b>Prefilter BW, R (<math>K_{bR}</math>)</b>	5.0	4.0
<b>Table 1: Gains used for Inner-Loop Control System</b>		
<b>Integral DI (<math>K_I</math>)</b>	0.5	0.5
<b>Anti-Windup, P (<math>K_{AW,P}</math>)</b>	0.2	0.1
<b>Anti-Windup, Q (<math>K_{AW,Q}</math>)</b>	0.2	0.1
<b>Anti-Windup, R (<math>K_{AW,R}</math>)</b>	0.2	0.1

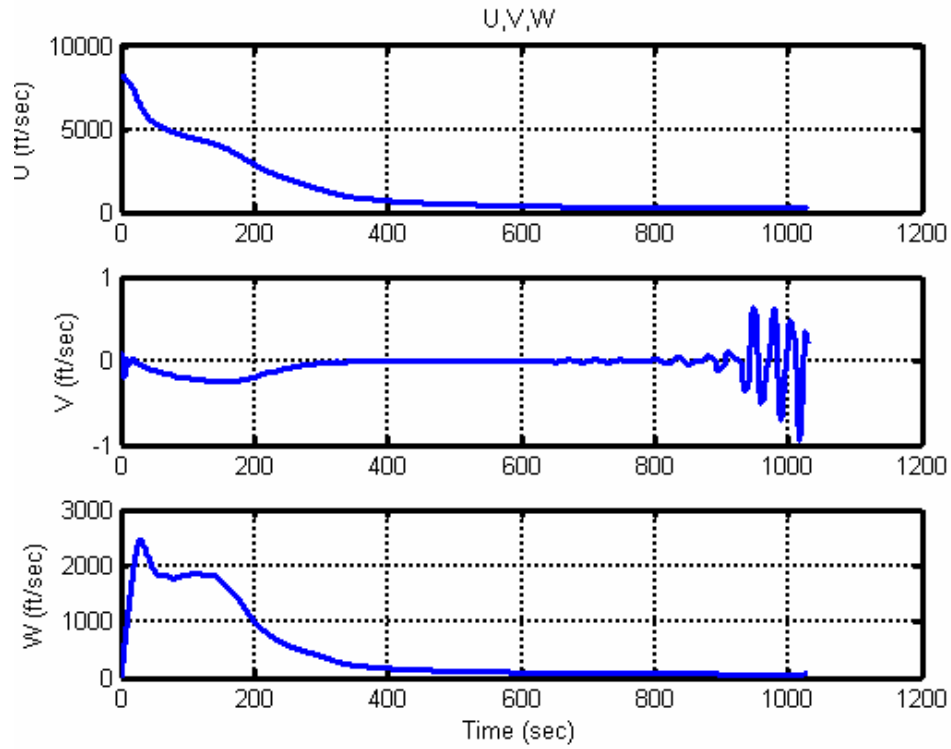


**Fig. 9: Max DR Linear Body-Relative Velocities (U,V,W)**

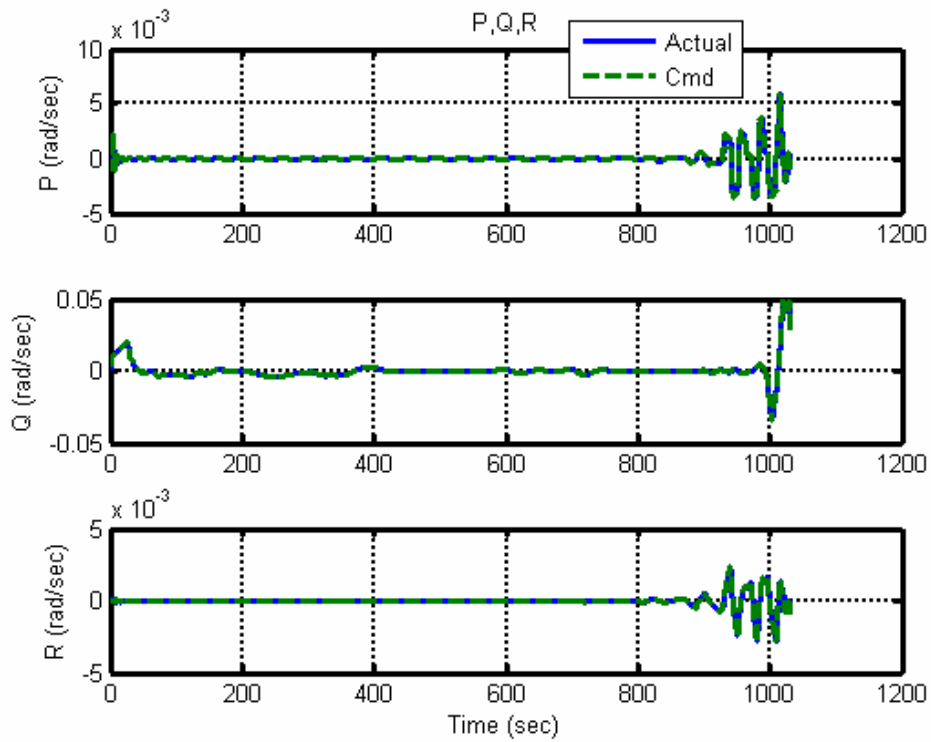


**Fig. 10: Max DR Angular Body-Rates (P,Q,R)**

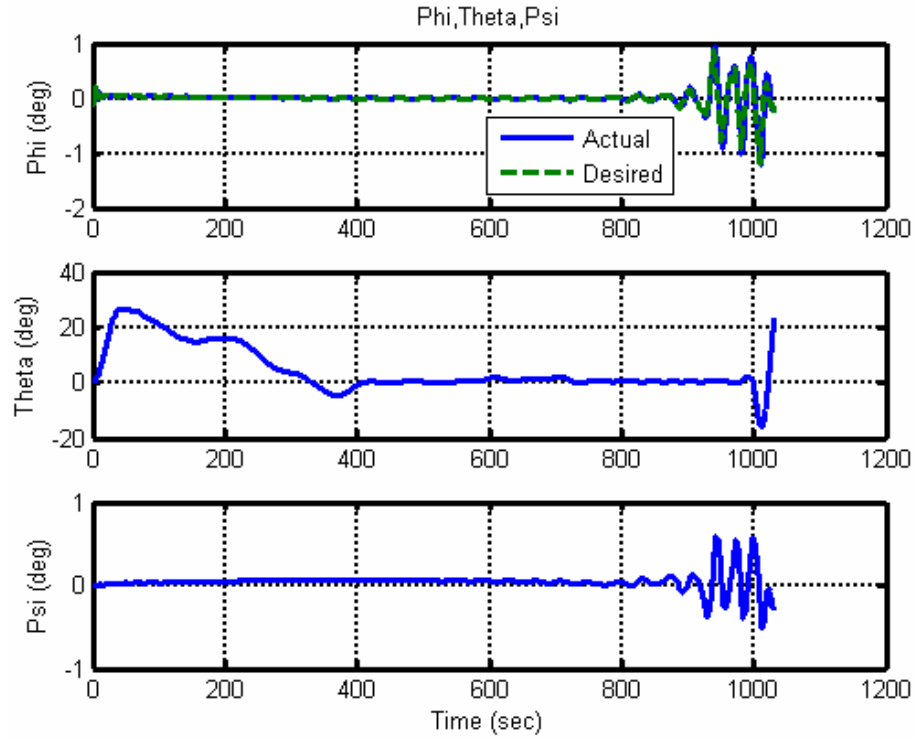


**Fig. 11: Max DR Euler Angles (Phi, Theta, Psi)**

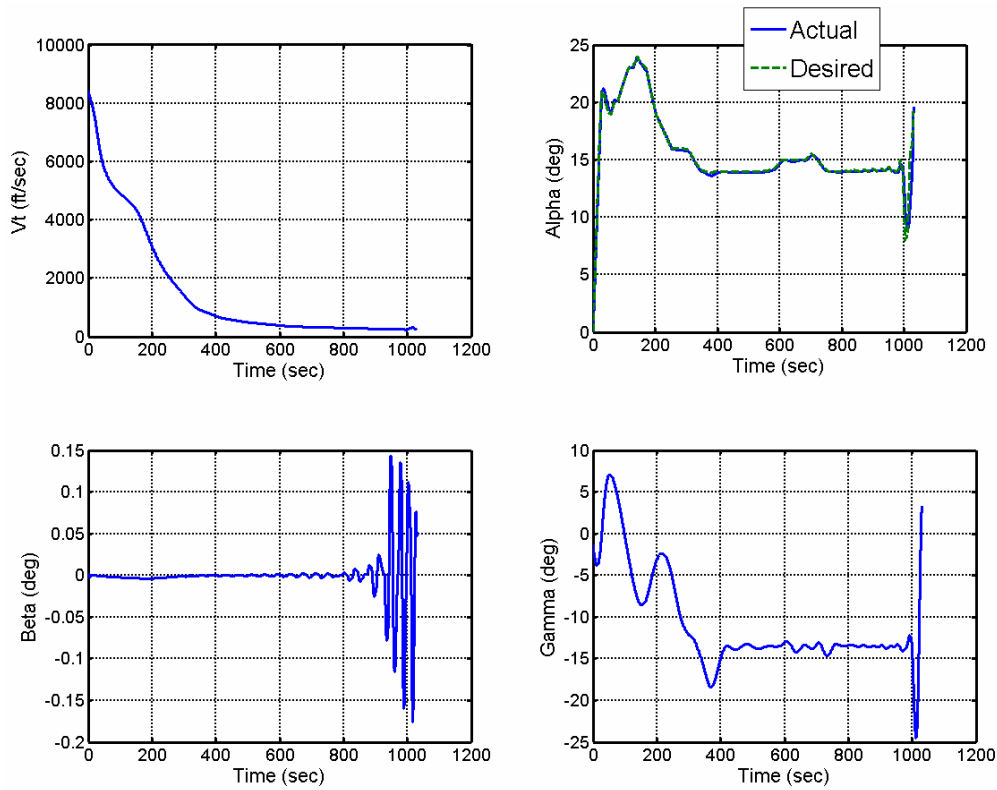


**Fig. 12: Max DR Airspeed (V) and Wind-Relative Angles (Alpha, Beta, Gamma)**

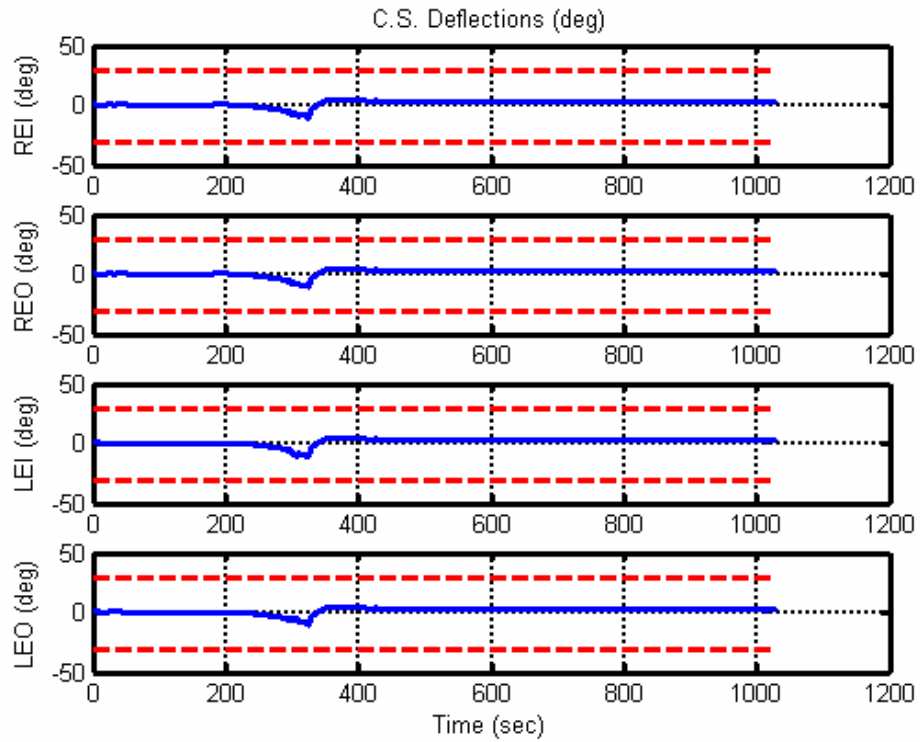


**Fig. 13: Max DR Elevon Control Surface Deflections**

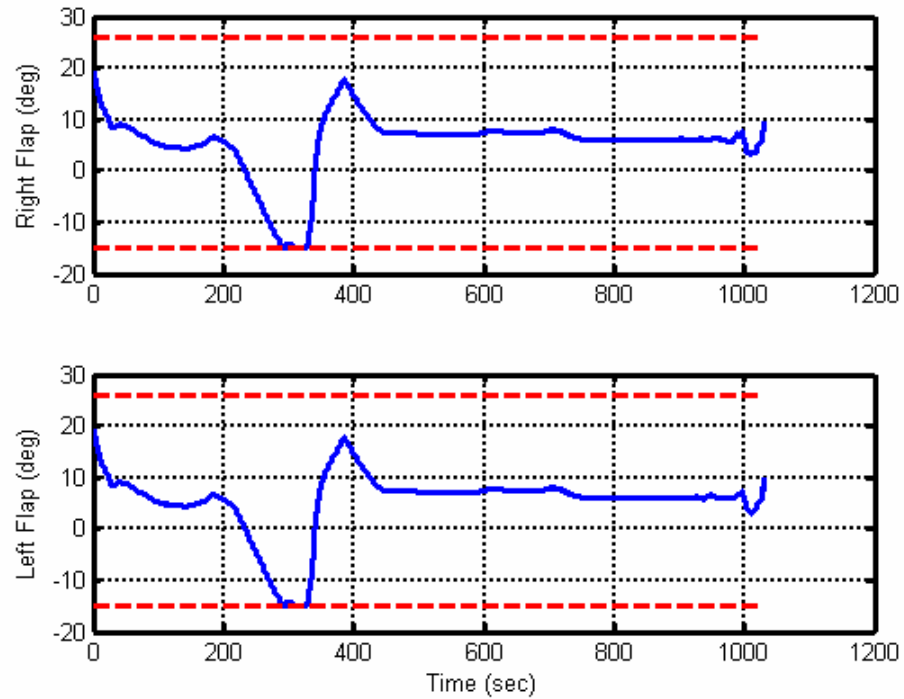


**Fig. 14: Max DR Body Flap Control Surface Deflections**

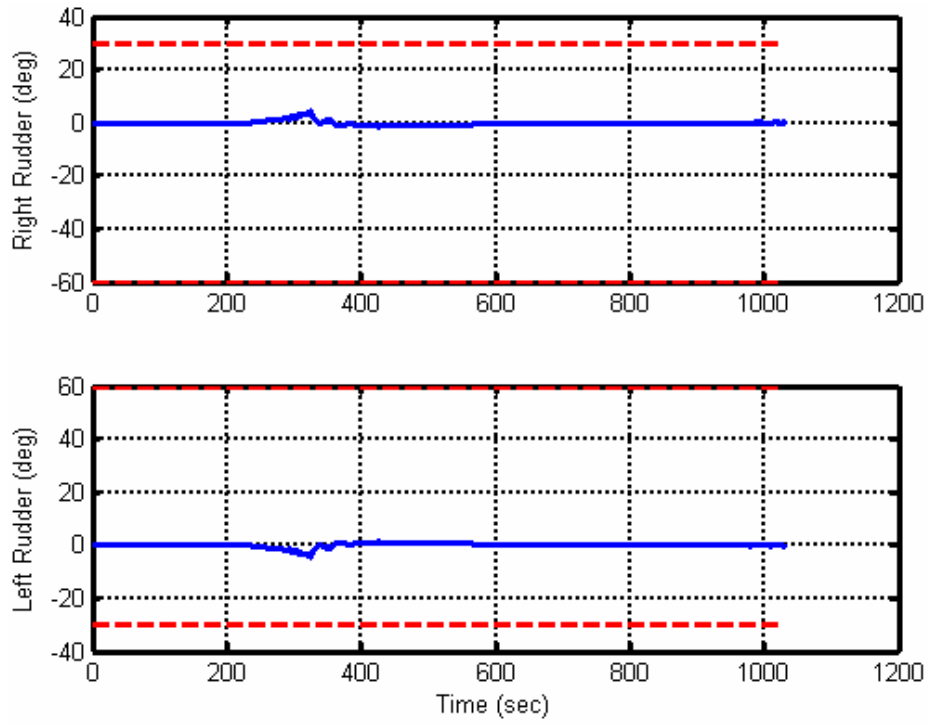


**Fig. 15: Max DR Rudder Control Surface Deflections**

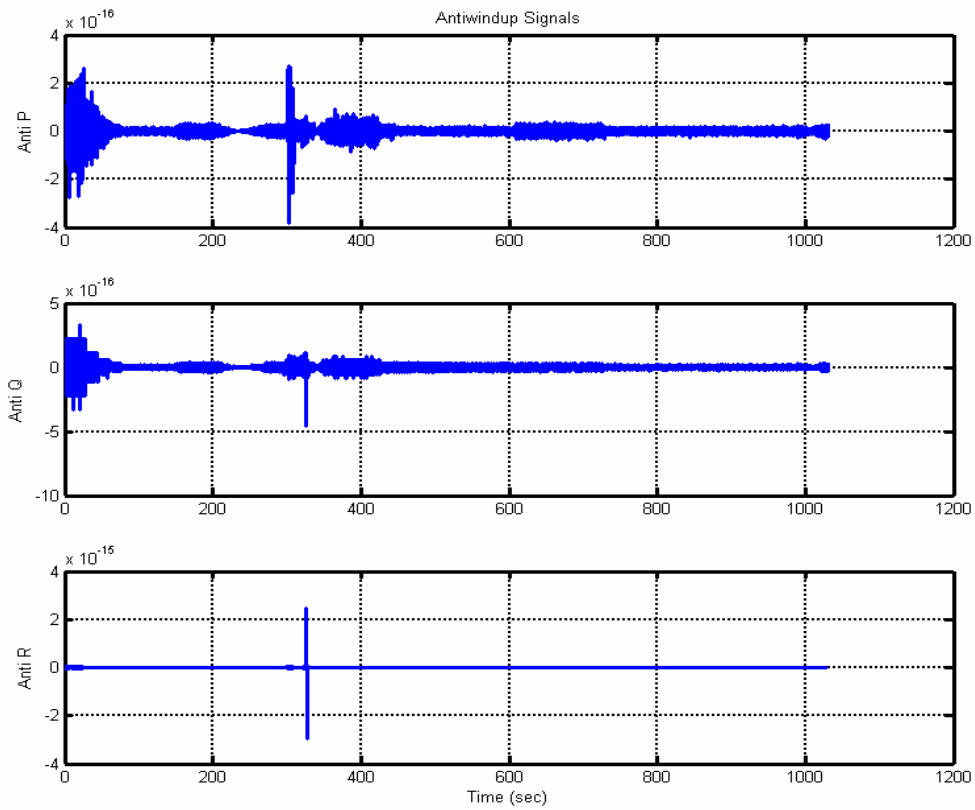


**Fig. 16: Max DR Anti-Windup Signals**

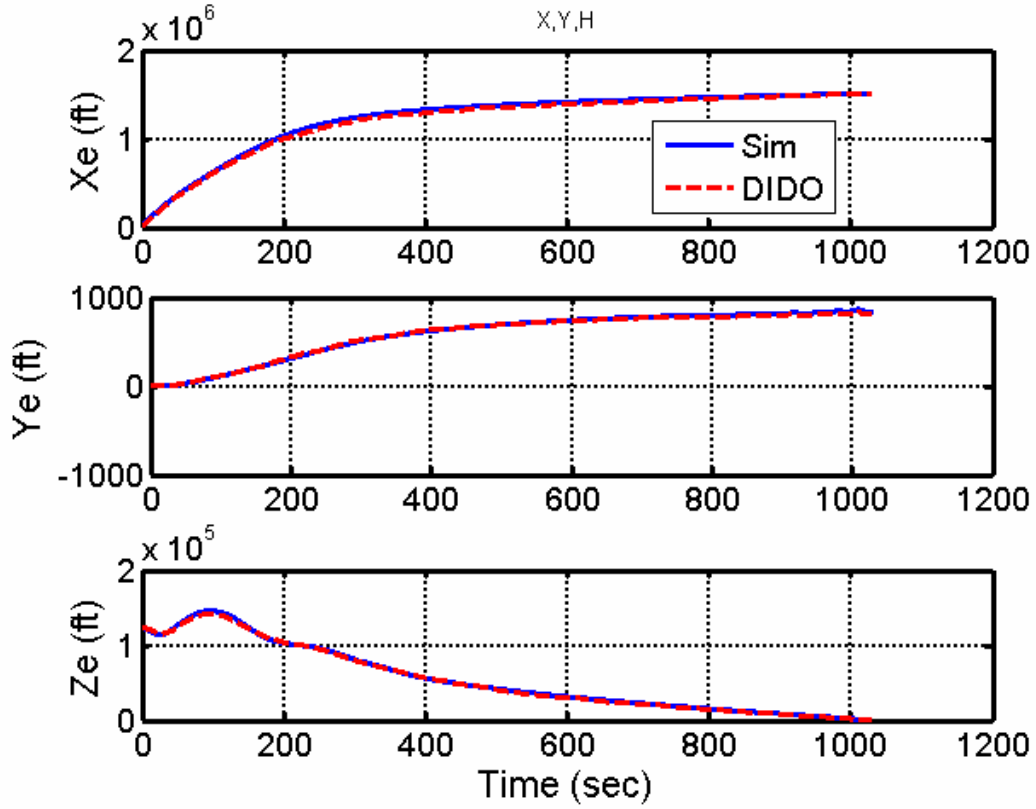
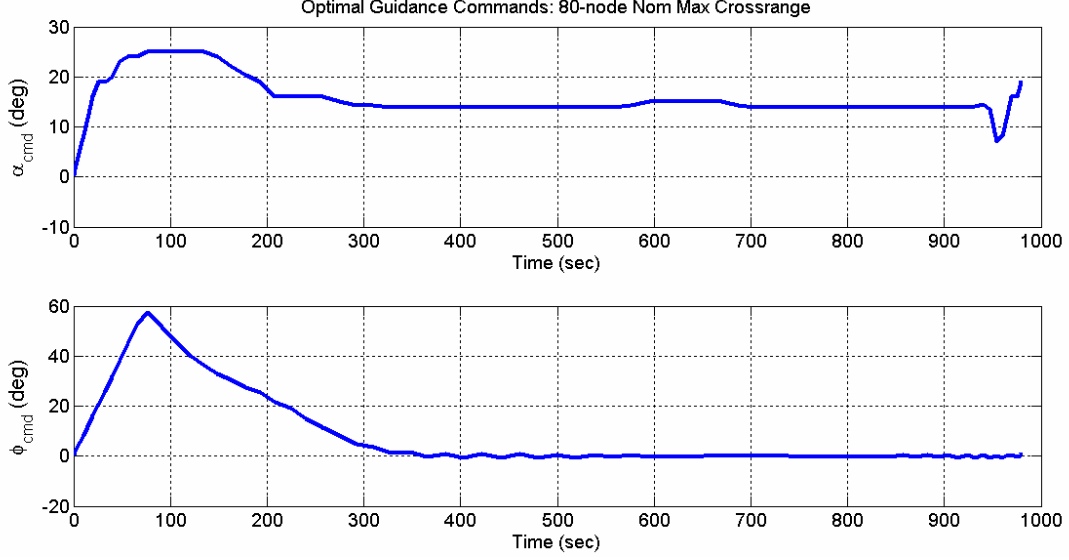


Fig. 17: Max DR Comparison of Reference and Tracking Trajectory

## 6.2. Max Cross-Range (CR) Case

For the case of maximizing the vehicle's cross-range distance,  $\alpha$  and  $\phi$  histories are extracted from the off-line optimal trajectory as was done for the max DR case. These commands are shown in Fig. 18.



**Fig. 18: Max CR Commands from 3-DOF Optimal Reference Trajectory**

For maneuvers with large bank angles, such as the max CR case, there is a loss of lift that must be countered in order to maintain altitude. Typically, the elevator is used to provide more lift. In short, the longitudinal and lateral equations of motion are strongly coupled during maneuvers with large bank angles. For example, a pilot must maintain adequate backpressure on the yoke during steep turns to prevent loss of altitude. To account for this in the pitch-command ( $Q_{cmd}$ ) generation, an extra lift term [28] was added to provide the appropriate contribution from the bank angle:

$$L = mg \sec(\phi) \Rightarrow \frac{g}{V} \sec(\phi) \quad (31)$$

With this addition and use of the gains in Table 1, the max CR results presented in Fig. 19 through Fig. 27 were acceptable with an average difference of only 2 %. The cost for the reference trajectory and the simulation were 664,862 ft and 671,781ft, respectively, which results in only a 1.04 % error.

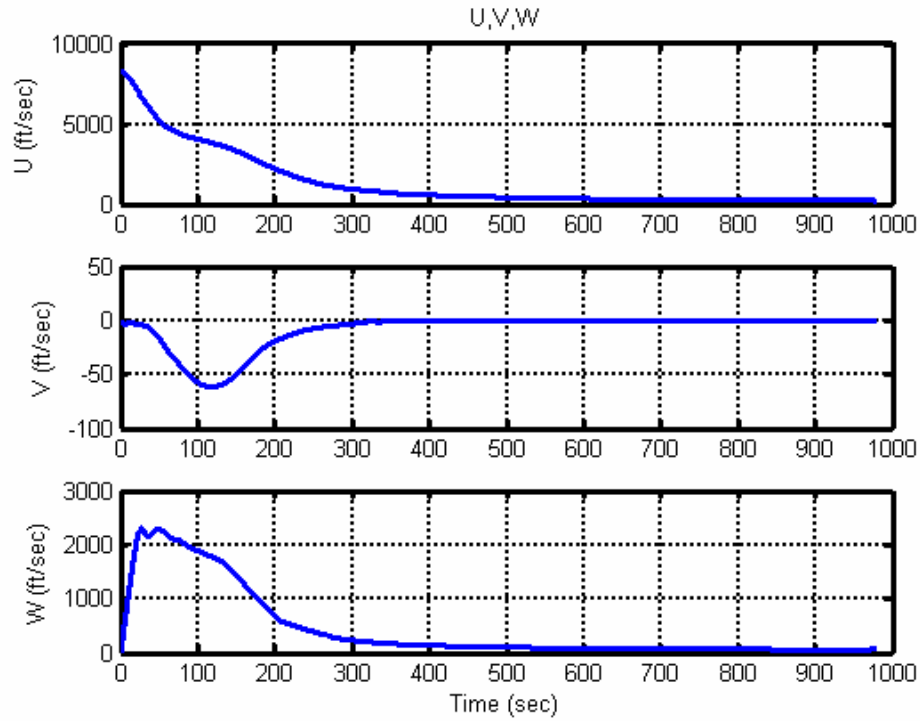


**Fig. 19: Max CR Linear Body-Relative Velocities (U,V,W)**

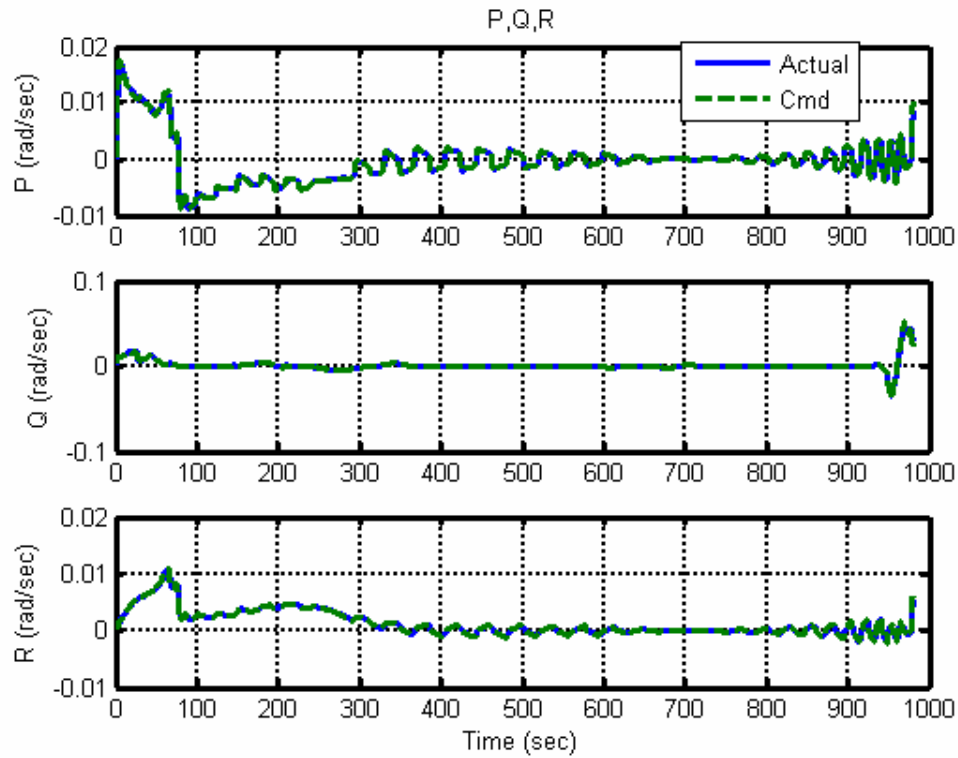


**Fig. 20: Max CR Angular Body-Rates (P,Q,R)**

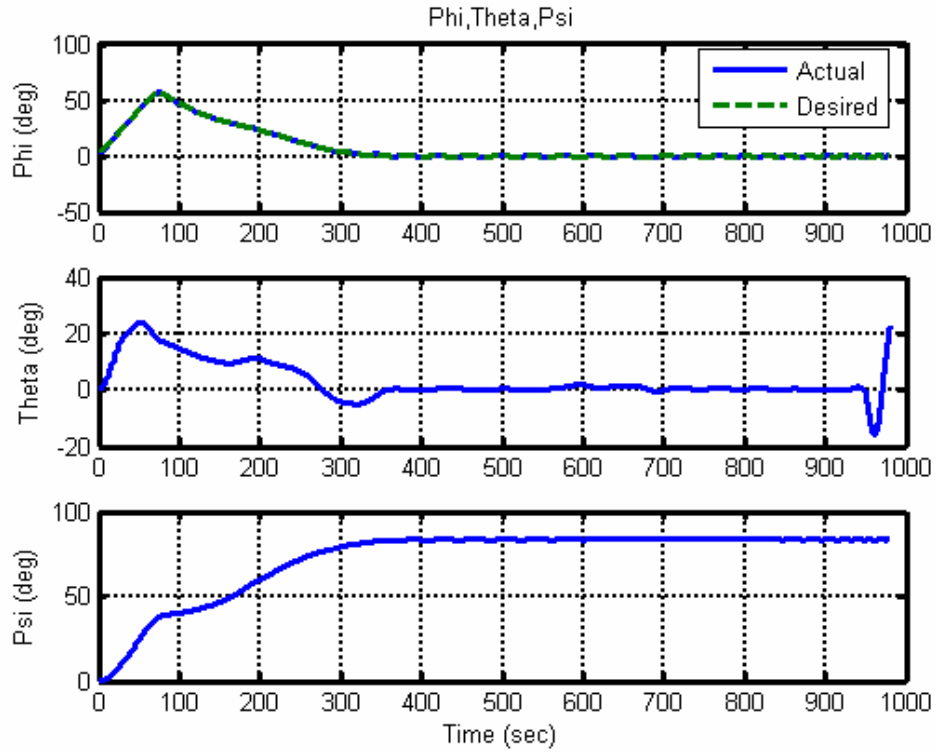


**Fig. 21: Max CR Euler Angles (Phi, Theta, Psi)**

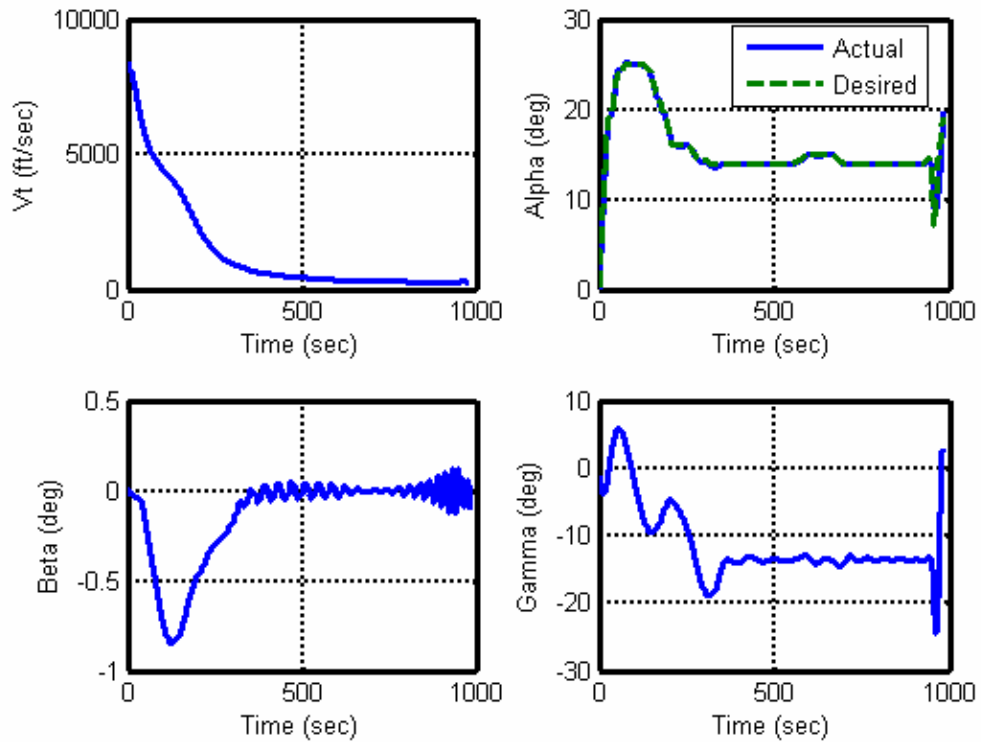


**Fig. 22: Max CR Airspeed (V) and Wind-Relative Angles (Alpha, Beta, Gamma)**

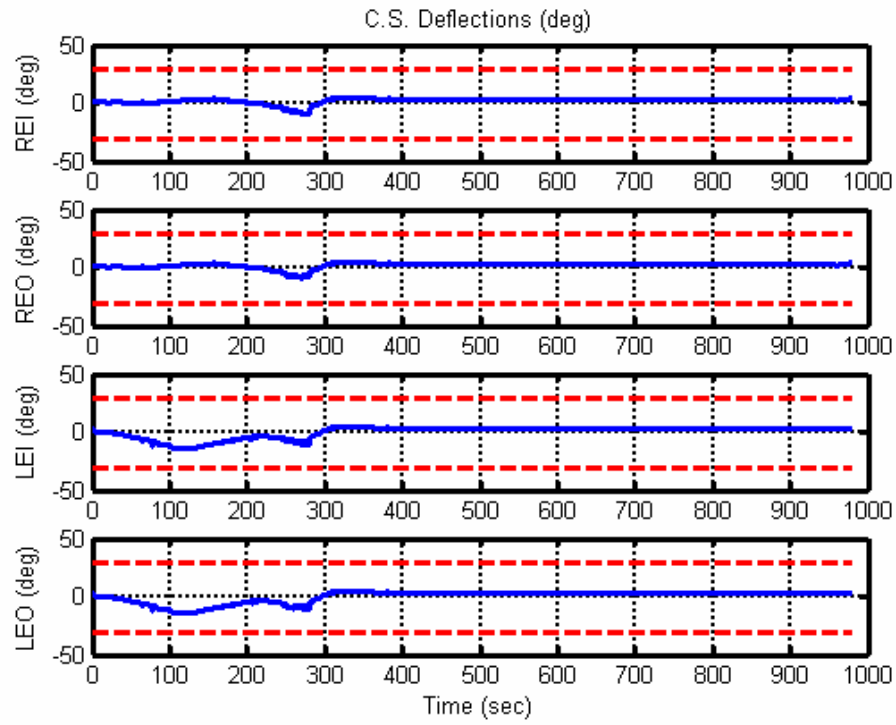


**Fig. 23: Max CR Elevon Control Surface Deflections**

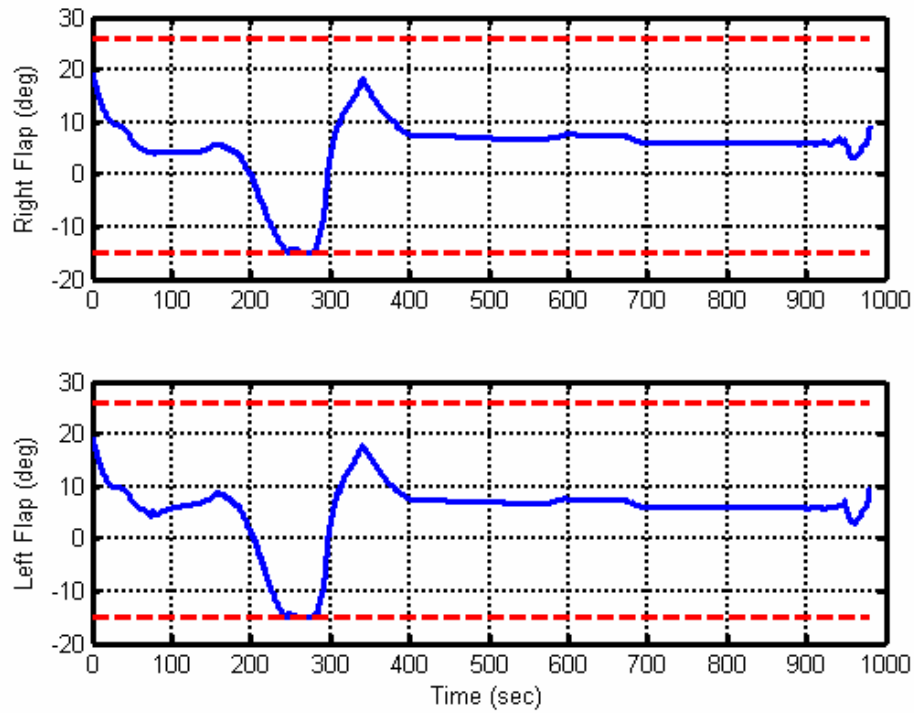


**Fig. 24: Max CR Body Flap Control Surface Deflections**

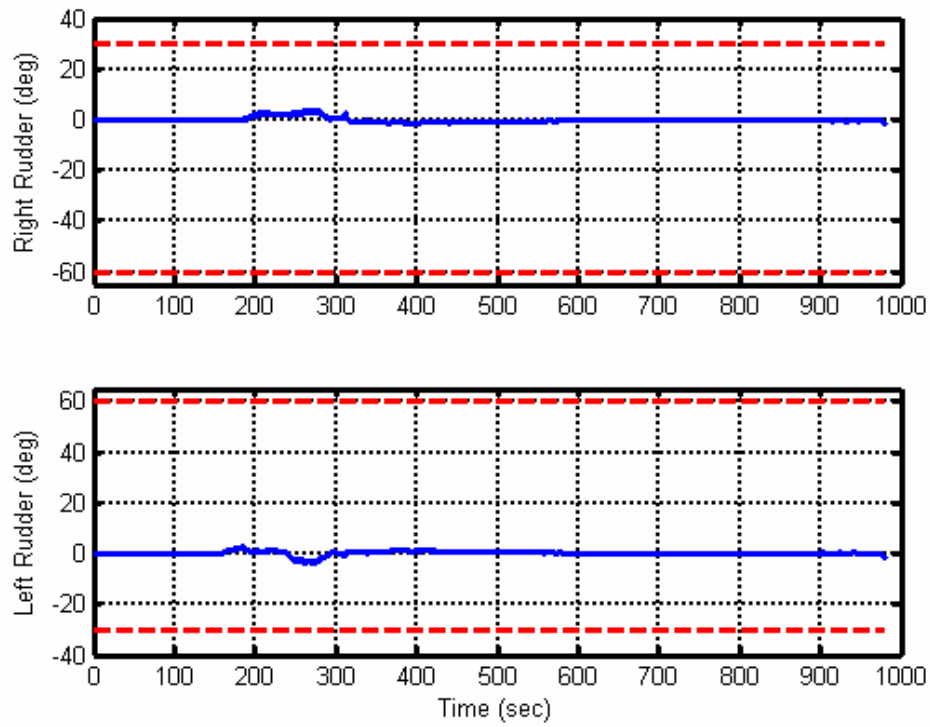


**Fig. 25: Max CR Rudder Control Surface Deflections**

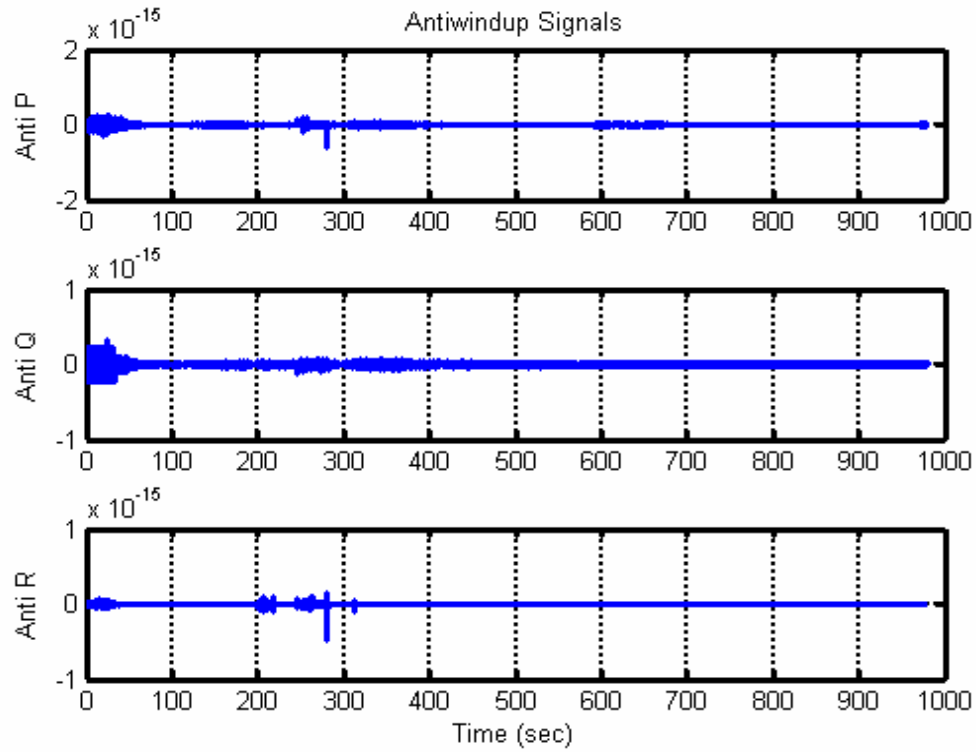


**Fig. 26: Max CR Anti-Windup Signals**

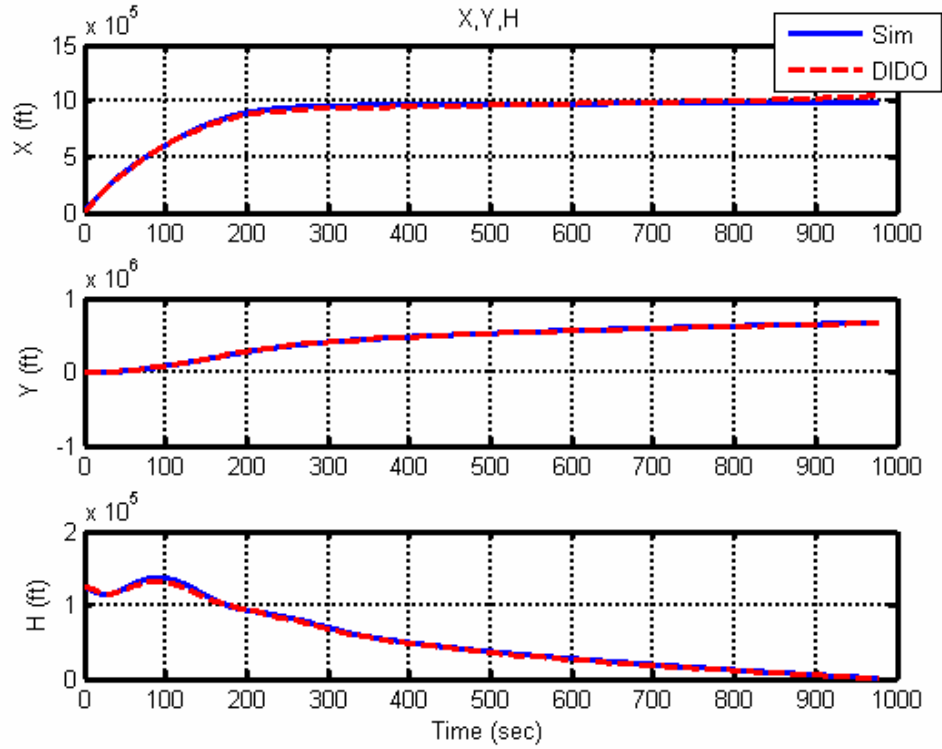


**Fig. 27: Max CR Comparison of Reference and Tracking Trajectory**

## 7. Conclusions

This paper presented successful integration of a reconfigurable inner-loop control law consisting of dynamic inversion, control allocation, model reference prefilters, and anti-windup integrators with an outer-loop, optimal guidance command generator. As demonstrated, the inner-loop control law was capable of tracking the body-frame angular rates that were converted from the wind-relative  $\alpha$  and  $\phi$  modulation of the off-line reference trajectory. Although the optimal trajectory generation was done off-line for this work, a similar model has already been demonstrated to work for on-line reentry applications using the same direct Legendre pseudospectral method.

The major drawback of the presented guidance and control architecture is that the inner-loop control system alone is not ideal for on-board autonomous applications. This control law requires various gains that would make strictly autonomous operations impractical, especially in situations involving unplanned maneuvers and/or flight anomalies. Even with the added robustness provided by the prefilters, anti-windup mechanism, and the optimal control allocation, an off-line gain schedule would still be required to handle the numerous unexpected operational conditions. With this said, concurrent and future work involves the use of on-line methods that can account for any unforeseen circumstances, including, but not limited to uncertain aerodynamics, significant external disturbances, control failures, and vehicle damage.

## 8. Acknowledgments

This work was sponsored by the Air Force Research Laboratory (AFRL/VACA), WPAFB, Ohio, under contract number FA9550-01-1-0001, with assistance provided by Dr. David Doman, the

Technical Area Leader for the Space Access and Hypersonic Vehicle Guidance and Control Group. His guidance on this work is greatly appreciated.

## References

1. Shaffer, P.J., Ross, I.M., Oppenheimer, M.W., Doman, D.B., "Optimal Trajectory Reconfiguration and Retargeting for a Reusable Launch Vehicle," *Proceedings of the 2005 AIAA Guidance, Navigation, and Control Conference*, AIAA Paper No. 2005-4168, Aug 2005.
2. Shaffer, Patrick J., *Optimal Trajectory Reconfiguration and Retargeting for the X-33 Reusable Launch Vehicle*, Thesis, Naval Postgraduate School, Monterey, CA, 2004.
3. Oppenheimer, M.W., and Doman, D.B., "Reconfigurable Control Design for the X-40A with In-Flight Simulation Results," *Proceedings of the 2005 AIAA Guidance, Navigation, and Control Conference*, AIAA Paper No. 2004-5017, Aug 2004.
4. Oppenheimer, M.W., and Doman, D.B., "Reconfigurable Inner Loop Control of a Space Maneuvering Vehicle," *Proceedings of the 2003 AIAA Guidance, Navigation, and Control Conference*, AIAA Paper No. 2003-5358, Aug 2003.
5. Doman, D.B., and Oppenheimer, M.W., "Integrated Adaptive Guidance and Control for Space Access Vehicles, Volume 1: Reconfigurable Control Law for X-40A Approach and Landing," *AFRL IAG&C Technical Report*, Wright-Patterson AFB, OH, 2004.
6. Pesch, H.J., "Off-Line and On-Line Computation of Optimal Trajectories in the Aerospace Field," Prepared for the 12<sup>th</sup> Course in *Applied Mathematics in the Aerospace Field* of the International School of Mathematics, Ettore Majorana Centre for Scientific Culture, Sicily, Sept 1991.
7. Shen, Z. and Lu, P., "Onboard Generation of Three-Dimensional Constrained Entry Trajectories," *Journal of Guidance, Control, and Dynamics*, Vol. 26, No. 1, pp.111-121, 2003.
8. Allwine, D.A., Fisher, J.E., Strahler, J.A., Lawrence, D.A., Oppenheimer, M.W., and Doman, D.B., "On-Line Trajectory Generation for Hypersonic Vehicles," *Proceedings of the 2005 AIAA Guidance, Navigation, and Control Conference*, AIAA Paper No. 2005-6435, Aug 2005.
9. Verma, A., Oppenheimer, M.W., and Doman, D.B., "On-Line Adaptive Estimation and Trajectory Reshaping," *Proceedings of the 2005 AIAA Guidance, Navigation, and Control Conference*, AIAA Paper No. 2005-6436, Aug 2005.
10. Schierman, J.D., Hull, J.R., and Ward, D.G., "On-Line Trajectory Command Reshaping for Reusable Launch Vehicles," *Proceedings of the 2003 AIAA Guidance, Navigation, and Control Conference*, AIAA Paper No. 2003-5439, Aug 2003.
11. Schierman, J.D., Hull, J.R., "In-Flight Entry Trajectory Optimization for Reusable Launch Vehicles," *Proceedings of the 2005 AIAA Guidance, Navigation, and Control Conference*, AIAA Paper No. 2005-6434, Aug 2005.
12. Harpold, J.C., and Graves, C.A., "Shuttle Entry Guidance," *The Journal of Astronautical Sciences*, Vol. 27, No. 3, pp.239-268, Jul-Sep 1979.
13. Schierman, J.D., Ward, D.G., Monaco, J.F., and Hull, J.R., "Reconfigurable Guidance Approach for Reusable Launch Vehicles," *Proceedings of the 2001 AIAA Guidance, Navigation, and Control Conference*, AIAA Paper No. 2001-4429, Aug 2001.

14. Schierman, J.D., Hull, J.R., and Ward, D.G., "Adaptive Guidance with Trajectory Reshaping for Reusable Launch Vehicles," *Proceedings of the 2002 AIAA Guidance, Navigation, and Control Conference*, AIAA Paper No. 2002-4458, Aug 2002.
15. Carson, J.M., Epstein, M.S., MacMynowski, D.G., and Murray, R.M., "Optimal Nonlinear Guidance With Inner-Loop Feedback for Hypersonic Re-Entry," Paper submitted to *American Control Conference*, 2005.
16. Bollino, K.P. and Ross, I.M., "Nonlinear Feedback Control for Rapid, On-line Trajectory Optimization of Reentry Vehicles," Submitted to *Proceedings of the 2006 AIAA Guidance, Navigation, and Control Conference*, AIAA Paper No. 2006-XXXX, Aug 2006.
17. Ross, I.M., and Fahroo, F., "Legendre Pseudospectral Approximations of Optimal Control Problems," *Lecture Notes in Control and Information Sciences*, Vol. 295, Springer-Verlag, new York, pp.327-342, 2003.
18. Ross, I.M., and Fahroo, F., "Pseudospectral Knotting Methods for Solving Optimal Control Problems," *Journal of Guidance, Control, and Dynamics*, Vol. 27, No. 3, pp.397-405, 2004.
19. Ross, I.M., Fahroo, F., and Gong, Q., "A Spectral Algorithm for Pseudospectral Methods in Optimal Control," *Proceedings of the 6<sup>th</sup> IASTED International Conference on Intelligent Systems and Control*, Honolulu, HI, 2004.
20. Ross, I.M., and Fahroo, F., "User's Manual for DIDO 2002: A MATLAB Application Package for Dynamic Optimization," NPS Technical Report AA-02-002, Department of Aeronautics and Astronautics, Naval Postgraduate School, Monterey, CA, June 2002.
21. Josselyn, S. and Ross, I.M., "Rapid Verification Method for the Trajectory Optimization of Reentry Vehicles," *Journal of Guidance, Control, and Dynamics*, Vol.26, No. 3, pp.505-508, 2002.
22. Fahroo, F., and Doman, D., "A Direct Method for Approach and Landing Trajectory Reshaping with Failure Effect Estimation," *Proceedings of the 2004 AIAA Guidance, Navigation, and Control Conference*, AIAA Paper No. 2004-4772, Aug 2004.
23. Schierman, J.D., Hull, J.R., Gandhi, N., and Ward, D.G., "Flight Test Results of an Adaptive Guidance System for Reusable Launch Vehicles," *Proceedings of the 2004 AIAA Guidance, Navigation, and Control Conference*, AIAA Paper No. 2004-4771, Aug 2004.
24. Bolender, M.A., and Doman, D.B., "Nonlinear Control Allocation Using Piecewise Linear Functions," *Journal of Guidance, Control, and Dynamics*, Vol.27, No. 6, pp.1017-1027, 2004.
25. Doman, D.B., and Oppenheimer, M.W., "Improving Control Allocation Accuracy for Nonlinear Aircraft Dynamics," *Proceedings of the 2002 AIAA Guidance, Navigation, and Control Conference*, AIAA Paper No. 2005-4667, Aug 2002.
26. Oppenheimer, M.W., and Doman, D.B., "Methods for Compensating for Control Allocator and Actuator Interactions," *Proceedings of the 2004 AIAA Guidance, Navigation, and Control Conference*, AIAA Paper No. 2004-5168, Aug 2004.
27. McLean, Donald, *Automatic Flight Control Systems*, Prentice Hall, Cambridge, 1990.
28. Etkin, Bernard, *Dynamics of Atmospheric Flight*, John Wiley & Sons, New York, 1972.